Quantitative proteomic analysis shows alterations in patient Rett syndrome iPSC cultures at early neuronal progenitor stages

Suzy Varderidou-Minasian
Universiteit Utrecht https://orcid.org/0000-0001-7879-4291
Lisa Hinz
VU medisch centrum
Dominique Hagemans
Universiteit Utrecht
Danielle Posthuma
VU medisch centrum
Maarten Altelaar
Universiteit Utrecht
Vivi M. Heine (vm.heine@amsterdamumc.nl)
https://orcid.org/0000-0003-4416-3875

Research

Keywords: Rett syndrome; iPSC; neuron differentiation; quantitative mass spectrometry; TMT-10plex

Posted Date: March 2nd, 2020

DOI: https://doi.org/10.21203/rs.3.rs-15527/v1

Version of Record: A version of this preprint was published at Molecular Autism on May 27th, 2020. See the published version at https://doi.org/10.1186/s13229-020-00344-3.

Abstract

Background

Rett syndrome (RTT) is a progressive neurodevelopmental disease that is characterized by abnormalities in cognitive, social and motor skills. RTT is often caused by mutations in the X-linked gene encoding methyl-CpG binding protein 2 (MeCP2). The mechanism by which impaired MeCP2 induces the pathological abnormalities in the brain is not understood. Both patients and mouse models have shown abnormalities at molecular and cellular level before typical RTT-associated symptoms appear. This implies that underlying mechanisms are already affected during neurodevelopmental stages.

Methods

To understand the molecular mechanisms involved in disease onset, we used an RTT patient induced pluripotent stem cell (iPSC)-based model with isogenic controls and performed time-series of proteomic analysis using in-depth high-resolution quantitative mass spectrometry during early stages of neuronal development.

Results

We provide mass spectrometry-based quantitative proteomic data, depth of about 7000 proteins, at neuronal progenitor developmental stages of RTT patient cells and isogenic controls. Our data gives evidence of proteomic alteration at early neurodevelopmental stages, suggesting alterations long before the phase that symptoms of RTT syndrome become apparent. We found changes in proteins involved in pathway associated with RTT phenotypes, including dendrite morphology and synaptogenesis. Differential expression increased from early to late neural stem cell phases, although proteins involved in immunity, metabolic processes and calcium signaling were affected throughout all stages analyzed.

Limitations

The limitation of our study is the number of biological replicates. As the aim of our study was to investigate a large number of proteins, only a limited amount of biological replicates were suitable for inclusions without reducing the number of target proteins. Therefore, larger sample sizes derived from RTT patients will be needed to validate results.

Conclusions

Our results provide a valuable resource of proteins to study potential targets for early treatment of RTT symptoms. We found consistent and time-point specific alterations during early neuronal differentiation in RTT cultures. Insight into altered protein levels can help development of new biomarkers and therapeutic approaches in RTT syndrome. Therefore, we hope that our results give awareness of the early pre-natal onset of RTT, providing new insights to explore early diagnosis and treatment.

Background

Rett syndrome (RTT) is a severe neurodevelopmental disorder that mainly affects females with a frequency of ~ 1:10,000 [1]. Clinical features of RTT start to present around 6–18 months of age, and include deceleration of head growth, abnormalities in cognitive, social and motor skill development and seizures [2, 3]. Postmortem studies showed increased density of neurons in combination with reduced soma sizes in RTT patient compared to healthy control brains [4, 5]. RTT neurons show a decrease in dendritic branching, and a reduced number of dendritic spines and synapses [6, 7]. While studies suggest affected neurodevelopment starting at early stages, the molecular mechanisms underlying neuropathology in RTT is not understood.

In 90–95% of the RTT cases, the disease is caused by dominant loss-of-function mutations in the X-linked gene encoding methyl-CpG binding protein 2 (MeCP2) [8]. Random X chromosome inactivation in females results in somatic mosaics with normal and mutant MECP2 [9]. Males carrying a MECP2 mutation are not viable or suffer from severe symptoms and die early in life [10]. MeCP2 is described as a nuclear protein modulating gene expression, via binding to methylated DNA and hundreds of target genes. These modulations take place through direct repression or activation of genes, or by means of DNA modulation and secondary gene regulation. Consequently, mutations in MECP2 lead to miss-regulation of hundreds of genes, including those influencing brain development and neuronal maturation [11–14]. So far research in RTT focused on genomic and transcriptomic studies [15–17] and less so on proteome changes [18, 19], although as molecular effectors of cellular processes, these are better predictors of pathological states. Recent advances in mass spectrometry-based proteomics now facilitate the study of global protein expression and quantification [20]. Considering the broad and complex regulating functions of MeCP2, modulating multiple cellular processes, we need insight into the final molecular effectors reflected by perturbation at the protein level to understand pathological states.

Here we used an iPSC-based RTT model and performed proteome analysis on iPSC-derived neuronal stem cells (NES cells) [21]. Earlier studies proved that iPSCs from RTT patients reflect disease-specific characteristics, including changes in neuronal differentiation at early stages of development [22, 23]. However, we lack knowledge on the precise molecular mechanisms at the onset of disease. To study early alterations in the proteome of RTT cells compared to isogenic controls (iCTR), we performed a high-resolution mass spectrometry-based quantitative proteomics at different time points during neuronal stem cell development (Fig. 1). We show that the difference between RTT and iCTR, in terms of the number of differentially expressed proteins, begins at early stages and increases at later progenitor stages. Interestingly, a large group of these proteins are involved in cellular processes, implicated in classical features of typical RTT phenotypes, such as dendrite formation and axonal growth. Proteins involved in immunity and metabolic processes are consistently changed between RTT and iCTR at all time points studied. Here we provide evidence of target proteins that could be explored as potential targets for early treatments to reduce progression of RTT symptoms.

Methods

Cell culture and isogenic controls

RTT patient fibroblasts were derived from the Cell lines and DNA bank of Rett syndrome, X-linked mental retardation and other genetic diseases at the University Siena in Italy via the Network of Genetic Biobanks Telethon. We used fibroblast lines carrying MECP2 mutation showing a deletion in Exon 3 and 4 of the MECP2 gene (RTT Ex3-4), (RTT#2282C2). Fibroblasts were derived frozen, thawed and expanded in fibroblast medium (DMEM-F12, 20% FBS, 1%NEAA, 1%Pen/Strep, 50 µM β-Mercaptoethanol). To generate pure RTT, i.e. cells expressing affected X-chromosome, and isogenic control, i.e. cells expressing the healthy X-chromosome, fibroblasts were detached from cell culture plate and single fibroblasts were seeded in a 96-well plate. Cells were further expanded and characterized for their MeCP2 state by immunocytochemistry and PCR [24]. All of our experiments were exempt from the approval of the institutional review board.

Reprogramming

Reprogramming of fibroblasts was performed as described before [24]. In brief, fibroblasts were detached from cell culture plate and washed with PBS. 4×10^5 cells were resuspended in 400 µl Gene Pulser® Electroporation Buffer Reagent (BioRad) with 23,4 µg of each episomal plasmid (Addgene, Plasdmid #27078, #27080, #27076) containing the reprogramming factors OCT4, SOX2, KLF4 and C-MYC. Cell solution was carefully mixed and electroporated with three pulses of 1.6 kV, capacitance of 3 µF and a resistance of 400 Ω (Gene Pulser II (BioRad)). Fibroblasts were left for recovery in Fibroblast medium without antibiotics containing 10 µM Rock inhibitor (Y-27632). After cells reached a confluence of 60–70%, medium was changed to TeSR™-E7™ (STEMCELL). Colonies appeared after 21–28 days. These were picked manually and maintained in TeSR™-E8™ (STEMCELL). iPSC lines were characterized for pluripotency [24]. Six iPSC lines derived from one individual were selected and used in the present study; three iCTR clones and three RTT Ex3-4 clones.

Differentiation of neuronal stem cells

The 6 iPSC lines were differentiated towards neuronal stem cells as described before [21, 25]. As described in the paper by Shi et al, this protocol of cortical neurogenesis follows the same temporal order as occurs in vivo. iPSCs were plated in high-density on Geltrex®-coated wells of a 12-well plate in TeSR™-E8™ with 10 µM Rock inhibitor. Medium was changed daily for 2 days. Afterwards half of the medium was changed daily with Neuro-Maintenance-Medium (NMM) (1:1 DMEM/F12 + GlutaMAX:Neurobasal Medium, 1x B27, 1xN2, 2.5 µg/mL Insulin, 1.5 mM L-Glutamin, 100 µM NEAA, 50 µM 2-Mercaptoethanol, 1% penicillin/streptomycin) containing 1 µM Dorsomorphin and 10 µM SB431542 up to day 12. At day 10–12 rosette structures appeared, which were manually picked and further cultured on Poly-L-Ornithin (0.01%)/Laminin (20 µg/ml) coated cell culture plates in NMM medium containing EGF (20 ng/ml) and FGF-2 (20 ng/ml). Half of medium was changed daily and cells were cultured up to day 22.

Immunocytochemistry

To perform immunocytochemistry, cells were fixated with 4% Paraformaldehyde and blocked with blocking buffer containing 5% Normal Goat Serum (Gibco®), 0.1% bovine serum albumin (SigmaAldrich) and 0.3% Triton X-100 (SigmaAldrich). Primary antibody incubation for MeCP2 (D4F3, CellSignaling, 1:200, rabbit), OCT3/4 (C-10, Santa Cruz, 1:1000, mouse), SSEA4 (Developmental Studies Hybridoma Bank, 1:50, mouse), TRA1-60 (Santa Cruz, 1:200, mouse), TRA1-81 (Millipore, 1:250, mouse), SOX2 (Millipore, 1:1000, rabbit) was performed in blocking buffer over night at 4 °C. Next day cells were washed and secondary antibody Alexa Fluor® 488 (ThermoFisher, 1:1000, mouse or rabbit) and Alexa Fluor® 594 (ThermoFisher, 1:1000, mouse or rabbit) were applied in blocking buffer for 1 h at room temperature. To identify cell nuclei DAPI was used for 5 min before cells were mounted with Fluoromount™ (Sigma-Aldrich).

RNA collection, Sequencing and PCR analysis

To isolate RNA samples, standard TRIzol®-Chloroform isolation was done. RNA was stored at -80 °C until further processing. For PCR analysis RT-PCR was performed. cDNA was synthesized by using SuperScriptIV-Kit (ThermoFisher) following manufacturer’s recommendations and could be stored until further processing at -20 °C. To perform PCR different primer sets were used (Table 1) and PCR was executed with Phire Hot Start II DNA Polymerase (ThermoFisher).

Table 1

Primers used for iPSC characterization.

OCT3/4	Fwd:	GAC AGG GGG AGG GGA GGA GCT AGG
	Rev:	CTT CCC TCC AAC CAG TTG CCC CAA AC
SOX2	Fwd:	GGG AAA TGG GAG GGG TGC AAA AGA GG
	Rev:	TTG CGT GAG TGT GGA TGG GAT TGG TG
NANOG	Fwd:	CAG CCC CGA TTC TTC CAC CAG TCC C
	Rev:	CGG AAG ATT CCC AGT CGG GTT CAC C
C-MYC	Fwd:	GCG TCC TGG GAA GGG AGA TCC GGA GC
	Rev:	TTG AGG GGC ATC GTC GCG GGA GGC TG
TDGF1	Fwd:	TGC TGC TCA CAG GGC CCG ATA CTT C
	Rev:	TCC TTT CGA GCT CAG TGC ACC ACA AAA C
UTF1	Fwd:	CAG ATC CTA AAC AGC TCG CAG AAT
	Rev:	GCG TAC GCA AAT TAA AGT CCA GA
DNMT3B	Fwd:	CAG GAG ACC TAC CCT CCA CA
	Rev:	TGT CTG AAT TCC CGT TCT CC
MECP2 (Set 1)	Fwd:	GGA GAA AAG TCC TGG AAG C
	Rev:	CTT CAC GGC TTT CTT TTT GG
MECP2 (Set 2)	Fwd:	CACGGAAGCTTAAGCAAAGG
	Rev:	CTGGAGCTTTGGGAGATTTG
EIF4G2	Rev:	CTT CAC GGC TTT CTT TTT GG
	Rev:	AGT TGT TTG CTG CGG AGT TGT CAT CTC GTC

Western blotting

Frozen cell pellets were lysed by adding WB-Lysate buffer (50 mM Hepes ph 7.5, 150 mM NaCl, 1 mM EDTA, 2.5 mM EGTA, 0.1% TritonX-100, 10% Glycerol, 1 mM DTT). To determine protein concentration Bradford-Test was performed and 30 µg of sample were used. For SDS-PAGE pre-casted Gels were used (Biorad) and ran in 10x Tris/Glycine Buffer for Western Blots and Native Gels (Biorad #1610734). Gels were blotted in tank-blotter (Biorad) on PVDF membranes (Biorad) according to manufactures protocol. After protein transfer blots were blocked in 5% BSA/TBS for 1 h and stained for SOX2 (1:100, Millipore AB5603), SOX9 (1:250; CellSignalling 82630) and ß-actin (1:1000; Chemicon, C4 MAB 1501) in 5% BSA/TBS over night at 4 °C. Next day blots were washed and stained with secondary antibodies in 5%

BSA/TBS for 1 h at room temperature. After another 3 TBS washes blots were stained with SuperSignal™ West Femto Maximum Sensitivity Substrate (ThermoFisher) and analysed with LiCor analyser.

Sample collection

Samples were collected at different days throughout the differentiation. First samples were taken at day 3 (D3) of protocol, one day after medium change towards NMM with Dorsomorphin and SB431542. Second samples were taken at day 9 (D9), before rosette structures were cut, reminiscent to the early stage of secondary neurulation [26] followed by third sample collection at day 15 (D15), after rosettes were manually picked, comparable to complete neural tube formation state. Finally, fourth samples were taken at day 22 (D22), after first passage was performed and cells were recovered. To collect, cells were washed once with PBS and then scraped off the cell culture plate. Solution was collected in an Eppendorf Microtube and centrifuged at maximum speed for 5 min. Supernatant was discarded and pellet was frozen at -80 °C until further processing for mass spectrometry.

Cell lysis and protein digestion

Samples were lysed, reduced and alkylated in lysis buffer (1% sodiumdeoxycholate (SDC), 10 mM tris(2-carboxyethyl)phosphine hydrochloride (TCEP), 40 mM chloroacetamide (CAA) and 100 mM TRIS, pH 8.0 supplemented with phosphatase inhibitor (PhosSTOP, Roche) and protease inhibitor (Complete mini EDTA-free, Roche). After sonication, samples were centifugated at 20,000 x g for 20 min. Protein concentration was estimated by a BCA protein assay. Reduction was done with 5 mM Ammonium bicarbonate and dithiothreitol (DTT) at 55 °C for 30 min followed by alkylation with 10 mM Iodoacetamide for 30 min in dark. Proteins were then digested into peptides by LysC (Protein-enzyme ratio 1:50) at 37 °C for 4 h and trypsin (Protein-enzyme ratio 1:50) at 37 °C for 16 h. Peptides were then desalted using C18 solid phase extraction cartridges (Waters).

Tandem Mass Tag (TMT) 10 plex labelling

Aliquots of ~ 100 µg of each sample were chemically labeled with TMT reagents (Thermo Fisher) according to Fig. 1. In total three TMT mixtures were created for each biological replicate. Peptides were resuspended in 80 µl resuspension buffer containing 50 mM HEPES buffer and 12.5% acetonitrile (ACN, pH 8.5). TMT reagents (0.8 mg) were dissolved in 80 µl anhydrous ACN of which 20 µl was added to the peptides. Following incubation at room temperature for 1 hour, the reaction was then quenched using 5% hydroxylamine in HEPES buffer for 15 min at room temperature. The TMT-labeled samples were pooled at 1:1 ratios followed by vacuum centrifuge to near dryness and desalting using Sep-Pak C18 cartridges.

Off-line basic pH fractionation

Before the mass spectrometry analysis, the TMT mixture was fractionated and pooled using basic pH Reverse Phase HPLC. Samples were solubilized in buffer A (5% ACN, 10 mM ammonium bicarbonate, pH 8.0) and subjected to a 50 min linear gradient from 18% to 45% ACN in 10 mM ammonium bicarbonate pH 8 at flow rate of 0.8 ml/min. We used an Agilent 1100 pump equipped with a degasser and a photodiode array (PDA) detector and Agilent 300 Extend C18 column (5 µm particles, 4.6 mm i.d., and

20 cm in length). The peptide mixture was fractionated into 54 fractions and consolidated into 20. Samples were acidified with 10% formic acid and vacuum-dried followed by re-dissolving in 5% formic acid/5% ACN for LC-MS/MS processing.

Mass spectrometry analysis

We used nanoflow LC-MS/MS using Orbitrap Lumos (Thermo Fisher Scientific) coupled to an Agilent 1290 HPLC system (Agilent Technologies). Trap column of 20 mm x 100 µm inner diameter (ReproSil C18, Dr Maisch GmbH, Ammerbuch, Germany) was used followed by a 40 cm x 50 µm inner diameter analytical column (ReproSil Pur C18-AQ (Dr Maisch GmbH, Ammerbuch, Germany). Both columns were packed in-house. Trapping was done at 5 µl/min in 0.1 M acetic acid in H_2O for 10 min and the analytical separation was done at 300 nl/min for 2 h by increasing the concentration of 0.1 M acetic acid in 80% acetonitrile (v/v). The mass spectrometer was operated in a data-dependent mode, automatically switching between MS and MS/MS. Full-scan MS spectra were acquired in the Orbitrap from m/z 350–1500 with a resolution of 60,000 FHMW, automatic gain control (AGC) target of 200,000 and maximum injection time of 50 ms. Ten most intense precursors at a threshold above 5,000 were selected with an isolation window of 1.2 Da after accumulation to a target value of 30,000 (maximum injection time was 115 ms). Fragmentation was carried out using higher-energy collisional dissociation (HCD) with collision energy of 38% and activation time of 0.1 ms. Fragment ion analysis was performed on Orbitrap with resolution of 60,000 FHMW and a low mass cut-off setting of 120 m/z.

Data processing

Mass spectra were processed using Proteome Discover (version 2.1, Thermo Scientific). Peak list was searched using Swissprot database (version 2014_08) with the search engine Sequest HT. The following parameters were used. Trypsin was specified as enzyme and up to two missed cleavages were allowed. Taxonomy was set for Homo sapiens and precursor mass tolerance was set to 50 p.p.m. with 0.05 Da fragment ion tolerance. TMT tags on lysine residues and peptide N termini and oxidation of methionine residues were set as dynamic modifications, and carbamidomethylation on cysteine residues was set as static modification. For the reporter ion quantification, integration tolerance was set to 20 ppm with the most confident centroid method. Results were filtered to a false discovery rate (FDR) below 1%. Finally, peptides lower than 6 amino-acid residues were discarded. Within each TMT experiment, reporter intensity values were normalized by summing the values across all peptides in each channel and then corrected for each channel by having the same summed value. After that the normalized S/N values were summed for all peptides. Finally proteins were Log_2 transformed and normalized by median subtraction. Proteins were included that are identified in 2 out of 3 replicates.

Data visualization

The software Perseus was used for data analysis and to generate the plots. Volcano plots for each time point was generated and up- or down-regulated proteins were considered significant with a fold change cut-off = 1.3. Functional analysis to enrich to GO terms were done on David Database and pathway

enrichment analysis was done on Reactome Functional Interaction (http://www.reactome.org/). Furthermore, protein interaction network was performed using Cytoscape, Gnenmania plugin.

Results

Generation of iPSC-derived neuronal progenitors from RTT and isogenic controls

RTT patient and iCTR fibroblasts were reprogrammed into iPSCs via electroporation of reprogramming plasmids [24]. Pluripotency was confirmed using classic assays, including immunocytochemistry (Additional file 1: Figure S1a) and RNA expression (Additional file 1: Figure S1b). Expression of mutated and healthy MeCP2 in the RTT and iCRT lines was confirmed by immunocytochemistry and PCR for MECP2 (Fig. 2a, b). Additionally, the protein expression level of MeCP2 detected by mass spectrometry showed a higher expression of MeCP2 in iCTR relative to RTT samples (Fig. 2c, Additional file 1: Figure S1c). A detectable low expression of mutant alleles, here MeCP2 expression in mutant RTT lines, is a common effect caused by the so-called co-isolation issue in TMT-experiments [27]. Generation of NES cells was performed as described before [21]. Neuronal induction into neuronal rosette structures was monitored by visual inspection, and appeared after approximately 12 days of neuronal development initiation (Fig. 1). Time points for sample collection were chosen along the differentiation towards neuronal progenitor cells.

MS-based quantitative proteomics during neuronal development

To study proteomic changes between RTT and iCTR during neuronal development, cell lysates at indicated time points were subjected to tryptic digestion, high-pH fractionation followed by high-resolution tandem mass spectrometry (LC-MS/MS) analysis and TMT-10plex quantification (Fig. 1). In total we identified up to 7702 proteins in total, of which 3658 proteins were identified in all samples (Additional file 1: Figure S2, Table S1). Next, to determine protein expression changes over time-points, we compared RTT versus iCTR and considered proteins involving p-value (smaller or equal to) ≤ 0.1 and (bigger or equal to) ≥ 1.3 fold change in 2 out of 3 biological replicates as significantly regulated (Fig. 3a, Table S2). This resulted in significantly up or down regulated proteins of 23 at D3, 111 at D9, 72 at D15, and 243 at D22, between RTT and iCTR. We then compared the significantly up or down regulated proteins across different time points as presented in a Venn diagram (Additional file 1: Figure S3). We noticed that the majority of the significantly regulated proteins only have 0–2% overlap between the different time points. To better understand what biological processes are involved at each time point, we performed Gene Ontology (GO) enrichment analysis with respect to biological functions (Fig. 3b). GO analysis on the significantly upregulated proteins in RTT versus iCTR revealed the GO terms ‘neuron apoptotic process’ and ‘cellular response to hypoxia’ at D3. GO terms related to down regulated proteins in RTT at D3 involved ‘negative regulation of axon regeneration’, ‘positive regulation of filopodium

assembly' and 'positive regulation of neuron projection development'. At D9, 'insulin receptor signaling pathway' was up regulated whereas 'excitatory postsynaptic potential' was down regulated in RTT. At D15, 'cell-cell adhesion' and 'acyl-CoA metabolic process' were up regulated and terms such as 'axon guidance', 'brain development' and 'histone acetylation' were down regulated. Furthermore, at D22, GO terms related to 'cell-cell adhesion' and 'actin cytoskeleton organization' were up regulated and 'nervous system development' and 'forebrain development' were down regulated in RTT. Terms such as brain development were down regulated in D15 as well as D22. Gene set enrichment analysis (GSEA) of all up and down regulated proteins further revealed that RTT associated proteins were strongly enriched in gene sets such as apoptosis, DNA repair and in metabolism (Additional file 1: Figure S4, Table S3). To further verify the results of the mass spectrometry, we performed western blot analysis for proteins SOX2 and SOX9, transcription factors with pivotal role in development and differentiation [28, 29], which showed significant differences in expression levels between iCTR and RTT lines at D22 (Fig. 3a, c). In line with mass spectrometry data, western blot analysis showed a significant increase in SOX9 expression levels in RTT lines when compared to iCTR ($p = 0.0057$, unpaired t-test), and a decrease in SOX2 expression in RTT lines at D22, although this did not reach statistical significance ($p = 0.07$, unpaired t-test). Together both approaches demonstrate that SOX2 and SOX9 were differentially expressed between RTT and iCTR, thereby validating our findings that RTT samples show proteome changes at early neurodevelopmental changes

A previous study identified perturbed astrocyte differentiation of RTT-iPSCs, suggesting skewed differentiation of neural progenitor cells into neuronal cell lineage [30]. Here we studied whether we could find similar changes, i.e. increased neuronal marker MAP2 and decreased glia marker (e.g. ATP1A2, CLU and SLC1A3) expression. While these astrocyte and neuronal markers are expressed in our samples, we found no significant differences between iCTR and RTT samples (Additional file 1: Figure S3). Furthermore, while the authors showed higher expression of LIN28 in RTT samples, we identified two isotopes (LIN28A and B) with no differences between RTT and iCTR samples. In addition, we compared our proteomic altered data to the Allen Brain atlas, which is showing individual gene expression in the different brain areas (Supplementary Table S4). This revealed high variability of expression between transcriptomics and proteomics. The majority of the proteins have measurable expression levels in human brain in vivo. Overall, we show that proteins associated with neuronal development are differentially expressed in RTT at early stages of neuronal differentiation.

Coordinated proteome alteration during neuronal development in RTT syndrome

To gain insight into how the differentially expressed proteins in RTT behave across time points, we further analysed all the significantly up or down regulated proteins at D3, D9, D15 and D22. This resulted in 234 significantly up and 190 down regulated proteins. The average log2 values of RTT were extracted with iCTR for each time point and the difference between RTT and iCTR is shown in a heat map (Fig. 4a). To obtain an unbiased view of the differentially expressed proteins during neuronal differentiation, we performed cluster analysis on the significantly up or down regulated proteins. This resulted in four

clusters for both the up or down regulated proteins with distinct expression profiles. Cluster 1 contains proteins strongly up regulated in D3 that are involved in neuron apoptotic processes and cytochrome c release from mitochondria-related GO terms. Cluster 2 represents up regulated proteins at D22 that are involved in adhesion assembly and glutathione metabolic processes. Cluster 3 contains proteins up regulated at D9 and D15 having a role in apoptotic signalling and cluster 4 represents proteins strongly up regulated at D9 having a role in oxidation and chromatin silencing. In the down regulated proteins, cluster 1 represents proteins that showed a strong down regulation at D15 mainly involved in cholesterol biosynthesis and fatty acid oxidation (Fig. 4b). Cluster 2 represents proteins strongly down regulated at D9, which are associated with regulation of proteolysis and mRNA stability. Cluster 3 of the down regulated proteins in RTT shows a decrease expression profile in D3 which are involved in axon regeneration and neuron projection development and cluster 4 covers many proteins strongly down regulated in D22 involved in processes such as neuronal stem cell maintenance, pituitary gland development and aging. Collectively, our data reveals a changing, stage-specific pattern of the differentially expressed proteins during neuronal development in RTT.

MeCP2 network analysis

To further investigate the proteins that are targets by the MeCP2 protein, we drew a protein interaction network (Cytoscape, Genemania plugin) using MeCP2 protein as input (Fig. 4c). The data covered 20 MeCP2-interacting proteins of which 18 proteins were identified in our data. To further investigate how the MeCP2- interacting proteins change over time in RTT, we extracted the average log2 values of iCTR by RTT samples to represents the difference at each time point. As expected, MeCP2 is down regulated along the course of neuronal differentiation in RTT samples compared to iCTR. The proteins are tightly interconnected around HDAC2, SIN3A, RBBP4, SAP30, SMARCE1, SMARCB1, and MeCP2, but to a lesser extend around CAT, XPC, PRPF40B, and MBD4. The network revealed several RNA/DNA binding proteins of which MeCP2 and CAT are one of the most down regulated proteins in RTT. While some proteins in the network, such as SMARCB1 and SIN3A stayed constant over time, others showed changing levels, such as MBD4 and HMGB1. Interestingly, MBD4, next to MeCP2, is a member of the methyl-CpG-binding domain (MBD) family. Overall, we searched for MeCP2-binding partners and showed how these proteins change along the course of neuronal differentiation in RTT and iCTR.

Protein subsets differentially expressed at all-time points

To study proteins differentially expressed between RTT and iCTR regardless the time point of differentiation, we grouped all RTT and all iCTR samples from all time points together. Due to the tight ratios typically observed in TMT quantification [31], we selected a cut-off for proteins being up or down regulated with a p-value ≤ 0.1 and ≥ 1.3 fold change difference in RTT compared to iCTR based on the observed distribution in the volcano plot (Fig. 5a). We identified 27 proteins being up and 12 proteins being down regulated in RTT compared to iCTR. As expected, MeCP2 was one of the most strongly down-regulated proteins in RTT. GO analysis revealed biological processes such as ‘cell-cell adhesion’ and ‘acyl-CoA metabolic processes’ to be up regulated (Fig. 5b), which are also up regulated at individual time

points D15 and D22 (Fig. 4a). In contrast, several processes such as ‘response to cadmium ion’, ‘response to drug’ and ‘behavioral fear response' were down regulated in RTT (Fig. 5b). Analysis of the differentially regulated proteins using Reactome pathway analysis revealed among others, ‘JAK/STAT signaling after Interleukin-12 stimulation’ and ‘regulation of MeCP2 expression and activity’ to be differentially expressed in RTT versus iCTR (Fig. 5c). To further visualize the connectivity among these significant proteins, we analyzed their protein networks in the Cytoscape tool (Genemania plugin). A high degree of connectivity, such as being co-expressed and having shared genetic interactions, around these proteins was identified. Interestingly, the majority of the proteins are involved in immunity, actin cytoskeleton organization and calcium binding (Fig. 5d). Together, we show that proteins associated with immunity and metabolic processes are differentially expressed in RTT in a time-point independent manner during differentiation towards neuronal progenitors.

Discussion

RTT samples present protein expression changes that became more apparent from early to late neuronal progenitor stages.

Already at D3 of neural induction, we found decreased protein levels associated with axon regeneration and filopodium assembly, and increased protein levels in neuronal apoptotic processes. Furthermore we show a down regulation of proteins associated with dendrite morphogenesis and excitatory postsynaptic potential at D9, and down regulation of axon guidance and brain development at D15 of neural induction. By D22 a clear set of proteins was altered in RTT with up regulated proteins associated with ‘cell adhesion’, ‘cytoskeleton organization’ and ‘translation initiation’. Proteins that are down regulated in RTT are involved in ‘nervous system development’, ‘forebrain development’ as well as ‘histone methylation’, which has classical roles with MeCP2 in its organization [32]. Previous study in MeCP2 deficient mice also found altered proteins associated to development and morphology of neurons as well as metabolism [33]. While the proteomic alterations found are relatively small (1.3 fold-change), they are in line with previous studies showing dysregulation of dendrites and axons in RTT patients/mouse models [34–37] as well as in the juvenile RTT brain [38–40]. Although neuronal progenitors did not develop dendrites or axons at these time points yet, our findings indicate that proteins involved in these processes are already expressed and altered in RTT at early developmental stages. During day 3–22, the number of proteins that are differentially expressed increases, although this set of protein changes over the time points. The increase of the fold change over time is an indicator of the manifestation of RTT, starting from early brain development towards the mature central nervous system. Furthermore, we noticed a small overlap of the altered proteins across time points which might indicate that proteins associated with RTT are specifically expressed at distinct time-points during the course of neural differentiation and reflect the robust cellular identity changes during early developmental stages. Proteins that are altered and could be used as targets for future treatments are DOCK6, NPC1, CDK5, HINT1, CSTB, ACSL4, KIF5C and TUBB2A. These proteins are identified to be dysregulated in other brain disorders such as epilepsy,

Niemann-Pick disease, mental retardation, cortical dysplasia, lissencephaly, neurotonia and axonal neuropathy. These candidate proteins need to be confirmed in other RTT cases as well before treatment therapy. Overall, we show that dysregulation of MeCP2 affects protein expression changes associated with neurodevelopmental functions at early stages of neuronal differentiation.

Expression changes of MeCP2-interacting proteins in RTT and iCTR

Network analysis using GeneMANIA [41] revealed part of these proteins to be interacting with MeCP2. Interestingly, of these interacting proteins, MBD4 is a member of the MBD family of proteins together with MeCP2. Mutations in these functional important domains tend to cause RTT-associated phenotypes [42–44]. Furthermore, HMGB1, which was down regulated in D9 and D15 in our data, was previously shown to be lower expressed in hippocampal granule neurons of Mecp2 KO mice [45].

Robust protein profile changes along the course of neuronal differentiation

When all RTT versus iCTR samples from different time points were pooled, data revealed differentially expressed proteins in RTT involved in immunity, calcium binding and metabolism. This analysis allowed us to compensate for limited amount of biological replicates in such high-throughput technology. Several proteins associated in metabolic processes were differentially expressed in RTT, including ACSF2, ACOT2, ACOT9, LDHA, MIF, NPC1, CAT and GSTO1. Current evidence in perturbed lipid metabolism in the brain and the peripheral tissue of RTT patients and mouse models now also supports the metabolic dysfunctions as a component of RTT [46]. Also mRNA GSTO1 was up regulated in RTT patients' lymphocytes together with several other mitochondrial related genes [47]. Furthermore, our results indicate dysregulated proteins associated with Interleuking-12 signalling. Interestingly, children with MECP2 duplication show immunological abnormalities and suppressed IFN-Y [48]. Although RTT is more often classified as a neurodevelopmental disorder, recent studies in cytokine release also suggest involvement of the immune system [49]. A previous study demonstrated that during early brain formation disturbances in the metabolism produces changes in the morphological and biochemical development of the brains [50]. Another study further observed that models with synaptic defects during development fail to couple to metabolic pathways [51]. These observation might indicate that the metabolic pathways could regulate the alterations in neuronal development. We further identified several proteins associated with calcium signalling to be altered. A disturbance in calcium homeostasis during early postnatal development was reported in Mecp2 knockout model and altered calcium signalling in RTT-iPSC-derived cells [52, 53]. Altogether, this indicates that next to dysregulation in neurodevelopmental processes, disease mechanisms underlying RTT phenotypes could also involve immunity, calcium signaling and metabolism.

Early treatment

The finding, that neuronal progenitor cells of RTT patients show altered protein expressions responsible for neuronal development and maturation, indicates that RTT influences the patients much earlier than first symptoms suggest. Therefore, early treatment should be explored. As there is no cure for RTT yet, mutations in MECP2 are not screened for in pre-natal diagnostics. However, early post-natal testing could still provide enough time to start treatment approaches, for example focused on supporting neuronal maturation with treatments, such as IGF-1 or Bumetanide [54–56], to extenuate disease symptoms. The progress of RTT is based on different aspects. There is evidence that mosaicism and therefore the ratio between cells expressing healthy compared to mutated MeCP2 plays a major role [57]. Furthermore, the mutation itself has a huge impact on severity of the disease [58]. However, in almost all cases of patients with MECP2 mutation a post-natal phase of compensation can be observed. In terms of diagnostics, mutations in MECP2 are not always associated with RTT and a mutation in MECP2 is not sufficient to make the diagnosis of RTT. RTT diagnosis is now based on clinical criteria rather than molecular findings. A set of altered signaling pathways or proteins, as found in this study, could be used as biomarkers to guide the disease diagnosis. Therefore, we hope that our results give awareness of the early pre-natal onset of RTT and could be further explored as potential targets for treatment.

Limitations

A limitation of our study is the number of biological replicates that was used (n = 3). Because of the incredible work that was needed, this number of replicates was feasible for this study. A possible avenue for future research would test few target proteins of a larger scale of biological replicates.

Conclusion

Before typical RTT-associated symptoms appear, both RTT patients and mouse models of RTT already show abnormalities [59, 60]. This implies that underlying mechanisms are already affected during early neurodevelopmental stages. Much of our understanding of how MeCP2 deficiency contributes to RTT disease is derived from genomic and transcriptomic studies. So far, only a few proteomic studies have been performed involving RTT human derived tissue [19, 61, 62]. The current study provides mass spectrometry-based quantitative proteomic data, depth of 7702 proteins, using an earlier developed iPSC-based models involving RTT patient and isogenic control cells [24]. We showed that changes in dendrite morphology or synaptic defects, previously associated with RTT [22, 63], already become apparent at early developmental stages. Proteins involved in immunity and metabolism, also in line with previous studies on RTT pathology [37, 46], are consistently differentially expressed at all time points studied. Insight into differentially expressed protein levels could support identification of novel biomarkers as well as therapeutic strategies.

Abbreviations

iPSC:induced pluripotent stem cell, MeCP2:methyl-CpG binding protein 2, RTT:Rett syndrome, iCTR:isogenic controls, GO:Gene ontology, TMT:Tandem mass tag,

Declarations

Acknowledgements

Specimens were provided by the Cell lines and DNA bank of Rett Syndrome, X-linked mental retardation and other genetic disease, member of the Telethon Network of Genetic Biobanks (project no. GTB12001), funded by Telethon Italy, and of the EuroBioBank network.

Funding

This work was funded by the EC under FP7-PEOPLE-2013 (607508) and The Netherlands Organization for Scientific Research (NWO VICI 453-14-005). VMH is supported by ZonMw (VIDI 917-12-343)

Ethics approval

All experiments were exempt from approval of Medical Ethical Toetsingscommissie (METC), Institutional Review Board of the VU medical centre.

Consent for publication

Not applicable

Competing interest

The authors declare that they have no competing interest

Data availability

All mass spectrometry proteomics data have been deposited to the ProteomeXchange Consortium via the PRIDE partner repository with the dataset identifier PXD013327
Username: reviewer46083@ebi.ac.uk
Password: ABIw2h3I

Authors contributions

S.V.M., L.H., M.A. and V.M.H. contributed to conception and design of the study. S.V.M. processed all mass spectrometry data and analysis. L.H. prepared all samples. D.H. helped with the cell lysis and TMT labeling. D.H., M.A. and V.M.H. contributed to acquisition. M.A. and V.M.H. supervised drafting final manuscript.

References

1. Chahrour, M. and H.Y. Zoghbi, *The story of Rett syndrome: from clinic to neurobiology.* Neuron, 2007. **56**(3): p. 422-37.
2. Neul, J.L., et al., *Rett syndrome: revised diagnostic criteria and nomenclature.* Ann Neurol, 2010. **68**(6): p. 944-50.
3. Percy, A.K., et al., *Rett syndrome diagnostic criteria: lessons from the Natural History Study.* Ann Neurol, 2010. **68**(6): p. 951-5.
4. Akbarian, S., *The neurobiology of Rett syndrome.* Neuroscientist, 2003. **9**(1): p. 57-63.

5. Marchetto, M.C., B. Winner, and F.H. Gage, *Pluripotent stem cells in neurodegenerative and neurodevelopmental diseases.* Hum Mol Genet, 2010. **19**(R1): p. R71-6.
6. Qiu, Z., et al., *The Rett syndrome protein MeCP2 regulates synaptic scaling.* J Neurosci, 2012. **32**(3): p. 989-94.
7. Smrt, R.D., et al., *Mecp2 deficiency leads to delayed maturation and altered gene expression in hippocampal neurons.* Neurobiol Dis, 2007. **27**(1): p. 77-89.
8. Amir, R.E., et al., *Rett syndrome is caused by mutations in X-linked MECP2, encoding methyl-CpG-binding protein 2.* Nat Genet, 1999. **23**(2): p. 185-8.
9. Trappe, R., et al., *MECP2 mutations in sporadic cases of Rett syndrome are almost exclusively of paternal origin.* Am J Hum Genet, 2001. **68**(5): p. 1093-101.
10. Schanen, C. and U. Francke, *A severely affected male born into a Rett syndrome kindred supports X-linked inheritance and allows extension of the exclusion map.* Am J Hum Genet, 1998. **63**(1): p. 267-9.
11. Lewis, J.D., et al., *Purification, sequence, and cellular localization of a novel chromosomal protein that binds to methylated DNA.* Cell, 1992. **69**(6): p. 905-14.
12. Nan, X., et al., *Transcriptional repression by the methyl-CpG-binding protein MeCP2 involves a histone deacetylase complex.* Nature, 1998. **393**(6683): p. 386-9.
13. Chahrour, M., et al., *MeCP2, a key contributor to neurological disease, activates and represses transcription.* Science, 2008. **320**(5880): p. 1224-9.
14. Gabel, H.W., et al., *Disruption of DNA-methylation-dependent long gene repression in Rett syndrome.* Nature, 2015. **522**(7554): p. 89-93.
15. Rodrigues, D.C., et al., *MECP2 Is Post-transcriptionally Regulated during Human Neurodevelopment by Combinatorial Action of RNA-Binding Proteins and miRNAs.* Cell Rep, 2016. **17**(3): p. 720-734.
16. Shovlin, S. and D. Tropea, *Transcriptome level analysis in Rett syndrome using human samples from different tissues.* Orphanet J Rare Dis, 2018. **13**(1): p. 113.
17. Colak, D., et al., *Genomic and transcriptomic analyses distinguish classic Rett and Rett-like syndrome and reveals shared altered pathways.* Genomics, 2011. **97**(1): p. 19-28.
18. Matarazzo, V. and G.V. Ronnett, *Temporal and regional differences in the olfactory proteome as a consequence of MeCP2 deficiency.* Proc Natl Acad Sci U S A, 2004. **101**(20): p. 7763-8.
19. Cortelazzo, A., et al., *A plasma proteomic approach in Rett syndrome: classical versus preserved speech variant.* Mediators Inflamm, 2013. **2013**: p. 438653.
20. Altelaar, A.F.M., J. Munoz, and A.J.R. Heck, *Next-generation proteomics: towards an integrative view of proteome dynamics.* Nature Reviews Genetics, 2012. **14**: p. 35.
21. Nadadhur, A.G., et al., *Multi-level characterization of balanced inhibitory-excitatory cortical neuron network derived from human pluripotent stem cells.* PLoS One, 2017. **12**(6): p. e0178533.
22. Andoh-Noda, T., et al., *Differentiation of multipotent neural stem cells derived from Rett syndrome patients is biased toward the astrocytic lineage.* Mol Brain, 2015. **8**: p. 31.

23. Kim, K.C., et al., *MeCP2 Modulates Sex Differences in the Postsynaptic Development of the Valproate Animal Model of Autism.* Mol Neurobiol, 2016. **53**(1): p. 40-56.
24. Hinz, L., et al., *Generation of Isogenic Controls for In Vitro Disease Modelling of X-Chromosomal Disorders.* Stem Cell Reviews and Reports, 2018.
25. Shi, Y., P. Kirwan, and F.J. Livesey, *Directed differentiation of human pluripotent stem cells to cerebral cortex neurons and neural networks.* Nature Protocols, 2012. **7**: p. 1836.
26. Fedorova, V., et al., *Differentiation of neural rosettes from human pluripotent stem cells in vitro is sequentially regulated on a molecular level and accomplished by the mechanism reminiscent of secondary neurulation.* Stem Cell Res, 2019. **40**: p. 101563.
27. Altelaar, A.F., et al., *Benchmarking stable isotope labeling based quantitative proteomics.* J Proteomics, 2013. **88**: p. 14-26.
28. De Santa Barbara, P., et al., *Direct interaction of SRY-related protein SOX9 and steroidogenic factor 1 regulates transcription of the human anti-Mullerian hormone gene.* Mol Cell Biol, 1998. **18**(11): p. 6653-65.
29. Rizzino, A., *Sox2 and Oct-3/4: a versatile pair of master regulators that orchestrate the self-renewal and pluripotency of embryonic stem cells.* Wiley Interdiscip Rev Syst Biol Med, 2009. **1**(2): p. 228-236.
30. Kim, J.J., et al., *Proteomic analyses reveal misregulation of LIN28 expression and delayed timing of glial differentiation in human iPS cells with MECP2 loss-of-function.* PLoS One, 2019. **14**(2): p. e0212553.
31. Altelaar, A.F.M., et al., *Benchmarking stable isotope labeling based quantitative proteomics.* Journal of Proteomics, 2013. **88**: p. 14-26.
32. Martinez de Paz, A. and J. Ausio, *MeCP2, A Modulator of Neuronal Chromatin Organization Involved in Rett Syndrome.* Adv Exp Med Biol, 2017. **978**: p. 3-21.
33. Pacheco, N.L., et al., *RNA sequencing and proteomics approaches reveal novel deficits in the cortex of Mecp2-deficient mice, a model for Rett syndrome.* Mol Autism, 2017. **8**: p. 56.
34. Lee, L.J., V. Tsytsarev, and R.S. Erzurumlu, *Structural and functional differences in the barrel cortex of Mecp2 null mice.* J Comp Neurol, 2017. **525**(18): p. 3951-3961.
35. Armstrong, D.D., *Neuropathology of Rett syndrome.* Ment Retard Dev Disabil Res Rev, 2002. **8**(2): p. 72-6.
36. Johnston, M.V., et al., *Neurobiology of Rett syndrome: a genetic disorder of synapse development.* Brain Dev, 2001. **23 Suppl 1**: p. S206-13.
37. Kaufmann, W.E., M.V. Johnston, and M.E. Blue, *MeCP2 expression and function during brain development: implications for Rett syndrome's pathogenesis and clinical evolution.* Brain Dev, 2005. **27 Suppl 1**: p. S77-s87.
38. Armstrong, D.D., *Rett syndrome neuropathology review 2000.* Brain Dev, 2001. **23 Suppl 1**: p. S72-6.

39. Jellinger, K. and F. Seitelberger, *Neuropathology of Rett syndrome.* Am J Med Genet Suppl, 1986. **1**: p. 259-88.
40. Boggio, E.M., et al., *Synaptic determinants of rett syndrome.* Frontiers in synaptic neuroscience, 2010. **2**: p. 28-28.
41. Montojo, J., et al., *GeneMANIA Cytoscape plugin: fast gene function predictions on the desktop.* Bioinformatics, 2010. **26**(22): p. 2927-8.
42. Moretti, P. and H.Y. Zoghbi, *MeCP2 dysfunction in Rett syndrome and related disorders.* Curr Opin Genet Dev, 2006. **16**(3): p. 276-81.
43. Shahbazian, M.D. and H.Y. Zoghbi, *Rett syndrome and MeCP2: linking epigenetics and neuronal function.* Am J Hum Genet, 2002. **71**(6): p. 1259-72.
44. Cukier, H.N., et al., *Novel variants identified in methyl-CpG-binding domain genes in autistic individuals.* Neurogenetics, 2010. **11**(3): p. 291-303.
45. Smrt, R.D., et al., *Mecp2 deficiency leads to delayed maturation and altered gene expression in hippocampal neurons.* Neurobiology of disease, 2007. **27**(1): p. 77-89.
46. Kyle, S.M., N. Vashi, and M.J. Justice, *Rett syndrome: a neurological disorder with metabolic components.* Open Biol, 2018. **8**(2).
47. Pecorelli, A., et al., *Genes related to mitochondrial functions, protein degradation, and chromatin folding are differentially expressed in lymphomonocytes of Rett syndrome patients.* Mediators Inflamm, 2013. **2013**: p. 137629.
48. Yang, T., et al., *Overexpression of methyl-CpG binding protein 2 impairs T(H)1 responses.* Sci Transl Med, 2012. **4**(163): p. 163ra158.
49. Leoncini, S., et al., *Cytokine Dysregulation in MECP2- and CDKL5-Related Rett Syndrome: Relationships with Aberrant Redox Homeostasis, Inflammation, and omega-3 PUFAs.* Oxid Med Cell Longev, 2015. **2015**: p. 421624.
50. Forrest, C.M., et al., *Kynurenine pathway metabolism following prenatal KMO inhibition and in Mecp2(+/-) mice, using liquid chromatography-tandem mass spectrometry.* Neurochem Int, 2016. **100**: p. 110-119.
51. Sullivan, C.R., et al., *Connectivity Analyses of Bioenergetic Changes in Schizophrenia: Identification of Novel Treatments.* Mol Neurobiol, 2019. **56**(6): p. 4492-4517.
52. Mironov, S.L., et al., *Remodelling of the respiratory network in a mouse model of Rett syndrome depends on brain-derived neurotrophic factor regulated slow calcium buffering.* J Physiol, 2009. **587**(Pt 11): p. 2473-85.
53. Marchetto, M.C., et al., *A model for neural development and treatment of Rett syndrome using human induced pluripotent stem cells.* Cell, 2010. **143**(4): p. 527-39.
54. Castro, J., et al., *Functional recovery with recombinant human IGF1 treatment in a mouse model of Rett Syndrome.* Proc Natl Acad Sci U S A, 2014. **111**(27): p. 9941-6.

55. Kahle, K.T., et al., *Decreased seizure activity in a human neonate treated with bumetanide, an inhibitor of the Na(+)-K(+)-2Cl(-) cotransporter NKCC1.* J Child Neurol, 2009. **24**(5): p. 572-6.
56. Tarquinio, D.C., et al., *Age of diagnosis in Rett syndrome: patterns of recognition among diagnosticians and risk factors for late diagnosis.* Pediatr Neurol, 2015. **52**(6): p. 585-91.e2.
57. Metcalf, B.M., et al., *Temporal shift in methyl-CpG binding protein 2 expression in a mouse model of Rett syndrome.* Neuroscience, 2006. **139**(4): p. 1449-60.
58. Cuddapah, V.A., et al., *Methyl-CpG-binding protein 2 (MECP2) mutation type is associated with disease severity in Rett syndrome.* J Med Genet, 2014. **51**(3): p. 152-8.
59. Charman, T., et al., *Regression in individuals with Rett syndrome.* Brain Dev, 2002. **24**(5): p. 281-3.
60. De Filippis, B., L. Ricceri, and G. Laviola, *Early postnatal behavioral changes in the Mecp2-308 truncation mouse model of Rett syndrome.* Genes Brain Behav, 2010. **9**(2): p. 213-23.
61. Cheng, T.-L., et al., *Regulation of mRNA splicing by MeCP2 via epigenetic modifications in the brain.* Scientific Reports, 2017. **7**: p. 42790.
62. Pecorelli, A., et al., *Proteomic analysis of 4-hydroxynonenal and nitrotyrosine modified proteins in RTT fibroblasts.* Int J Biochem Cell Biol, 2016. **81**(Pt B): p. 236-245.
63. Kim, K.Y., E. Hysolli, and I.H. Park, *Neuronal maturation defect in induced pluripotent stem cells from patients with Rett syndrome.* Proc Natl Acad Sci U S A, 2011. **108**(34): p. 14169-74.

Supplementary Files Legend

Additional file

Additional file 1: Figure S1. iPSC characterisation. **a**. Exemplary characterisation of iPSC lines. Immunocytochemistry for pluripotency marker (OCT3/4, SOX2, SSEA4, TRA1-60, TRA1-81). **b**. PCR-analysis for pluripotency marker. **c**. MeCP2 expression of the three iCTR and RTT samples at each time point.

Additional file 2: Figure S2. Number of proteins identified. A bar chart showing the number of proteins identified in each biological replicate and time point.

Additional file 3: Figure S3. Venn diagram. **a**. Number of proteins decreased expressed in RTT at different time points. **b**. Number of proteins increased expressed in RTT at different time points. **c**. Overview of the number of proteins altered in RTT.

Additional file 4: Figure S4. Top gene sets enriched in RTT-iPSCs. Proteins below p=0.1 are ranked by GSEA based on their differential expression level. Black vertical lines indicate the position where members of a pathway appear in the ranked gene list.

Figures

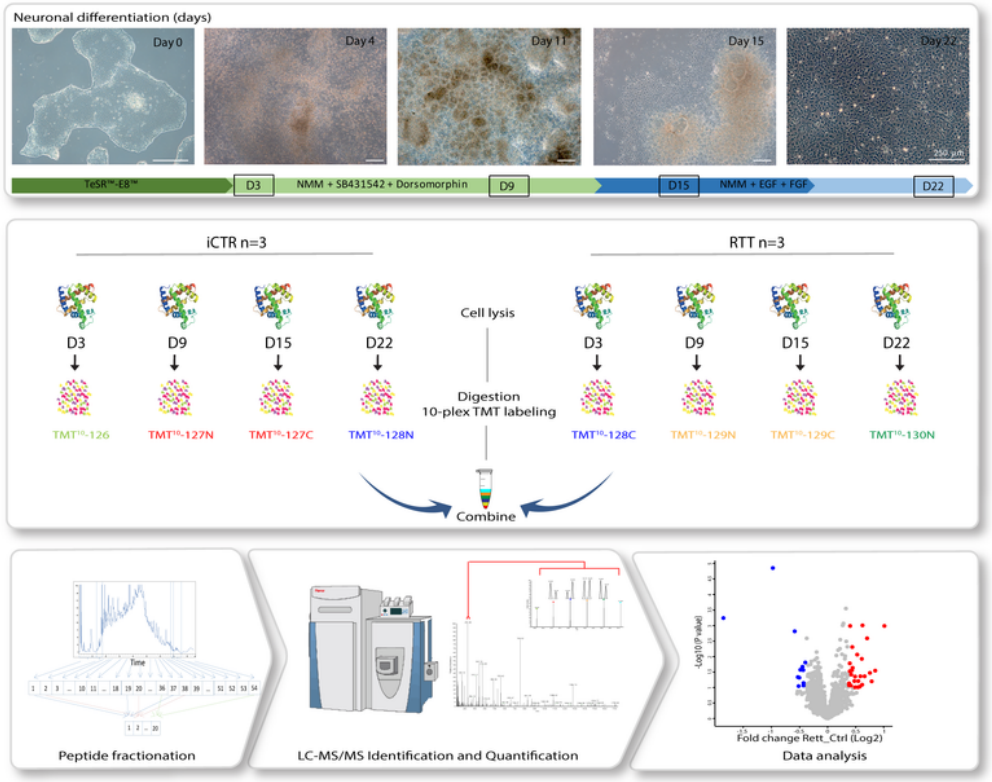

Figure 1

Overview of experimental workflow. iPSC differentiation towards neurons. Different colors in arrows indicate change of medium. Squares mark days of sample collection. Samples at indicated time points (four time points) for (three clones) iCTR and (three clones) RTT were processed for proteomic analysis. In total 24 samples were subjected for tryptic digestion, TMT-based isotope labeling, high-pH

fractionation and LC MS/MS analysis. Different bioinformatic approaches were then used to analyze the data.

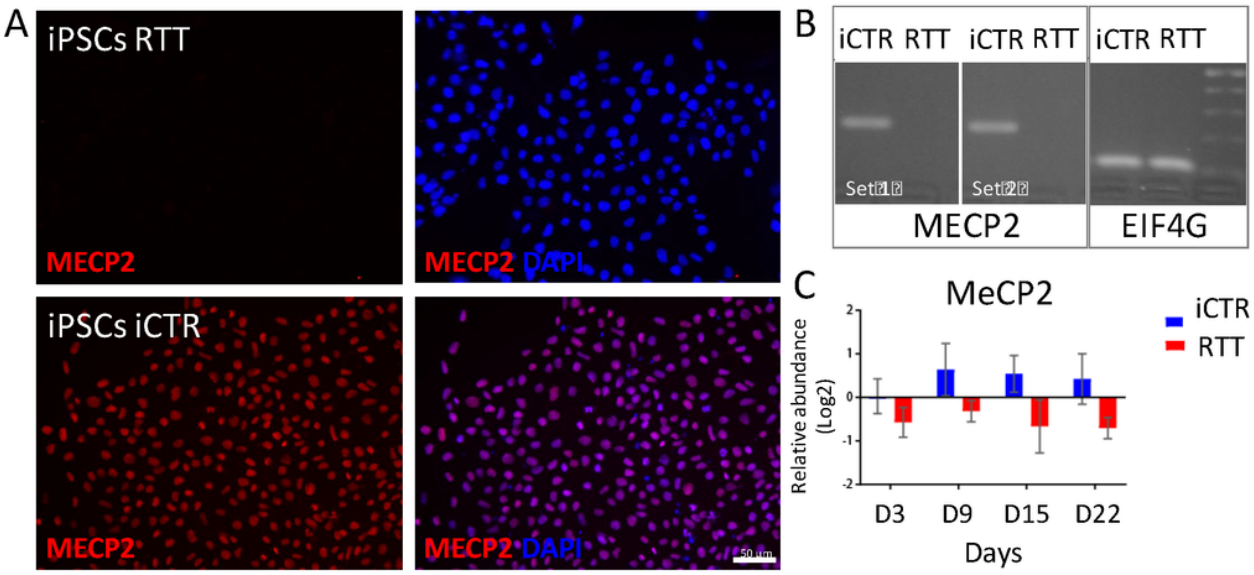

Figure 2

iCTR and RTT cell line validation. a. Representative immunohistochemical staining for MeCP2 in RTT iPSC line (upper) and iCTR iPSC line (lower). b. PCR results of iCTR and RTT iPSC lines for two different primer sets spanning deletion Del_Ex3-4 and Exon2 as positive control. c. Relative abundance level of MeCP2 in RTT NES and iCTR NES lines at different time points of sample collection.

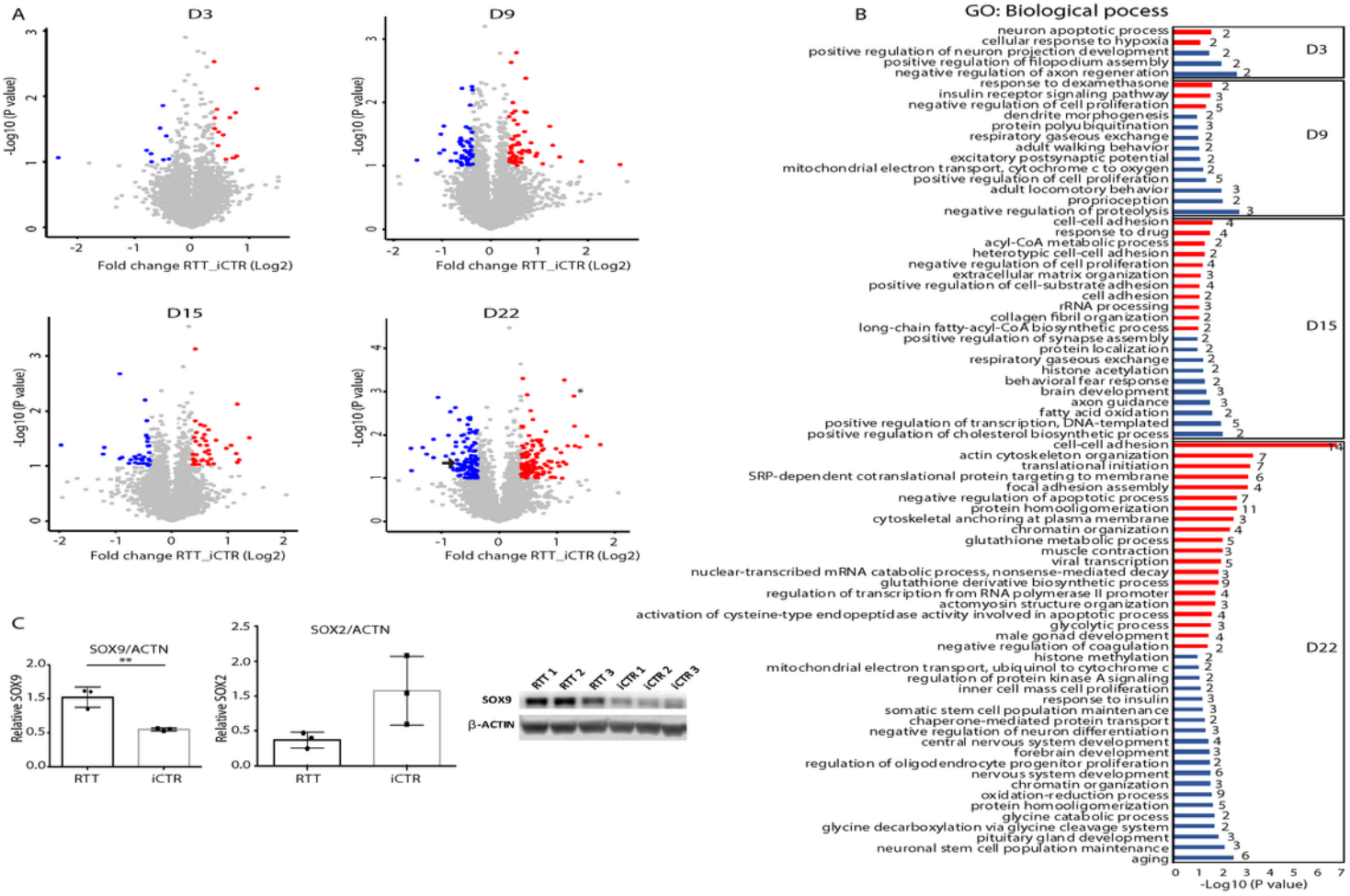

Figure 3

Volcano plots and GO analysis at different time points. a. Volcano plot demonstrating proteins differentially regulated in RTT compared to iCTR at each time point of neuronal development. Each data point represents a single quantified protein. The x-axis represents the log2-fold change in abundance (RTT/iCTR) and y-axis the -log10 (p-value). Threshold for significant proteins is chosen for p- value cut-off (0.1) and fold change ≥ 1.3. Proteins in blue indicate for down regulation and in red indicate for up

regulation in RTT. Arrow in day 22 points for SOX2 expression and asterisk points for SOX9 expression. b. Gene Ontology analysis of the significant proteins on their biological function at each time point of neuronal differentiation. Red indicates the up regulated and blue the down regulated biological processes. The numbers indicate the genes enriched for each term. c. Western blot analysis showing SOX9 and SOX2 expression in iCTR NES lines at D22. Significant increase in SOX9 expression in RTT samples and SOX2 shows a trend towards decrease in RTT samples.

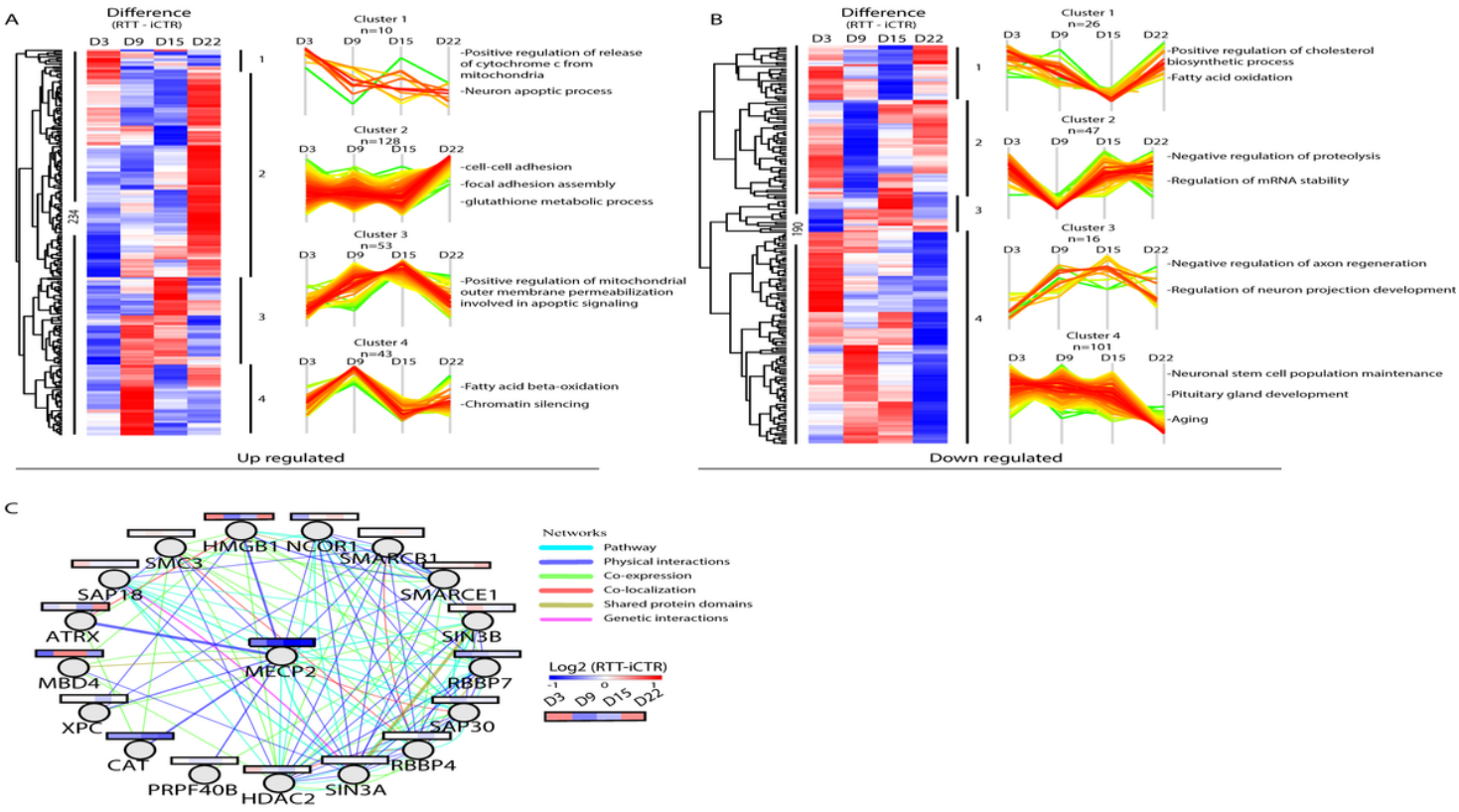

Figure 4

Up and down regulated proteins and MeCP2-binding partners. a. Heat map of all significant up and b. down regulated proteins with a p-value ≤ 0.1 and ≥ 1.3 fold change between RTT and iCTR. The Z score of the difference between RTT - iCTR is given for each day with the corresponding cluster analysis and the GO terms for biological processes. c. Network analysis of MeCP2-binding proteins identified in our

data. The average Log2 ratio RTT-iCTR over time is color coded for each protein over the time course of neuronal development. Edges are color coded according to the network as indicated.

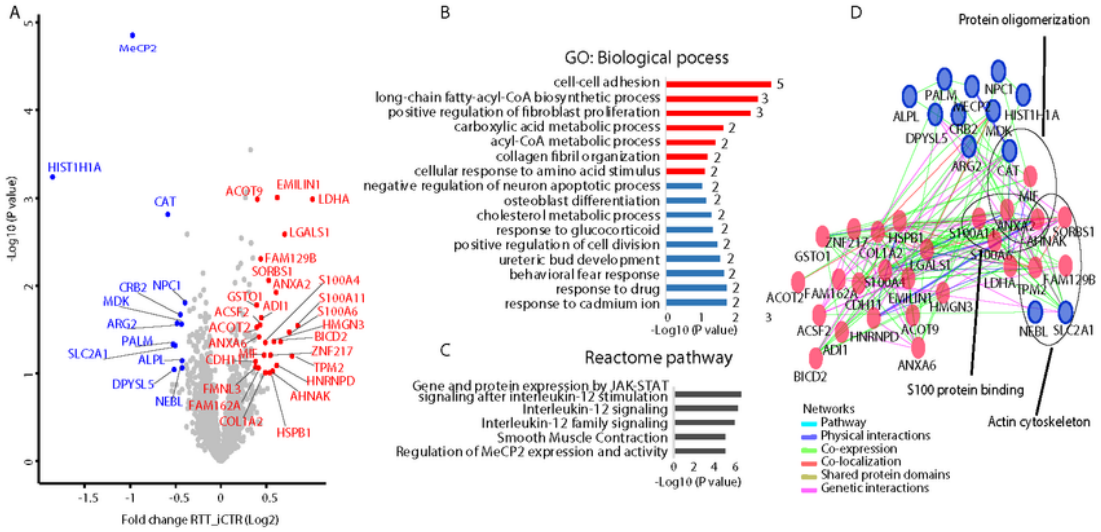

Figure 5

Volcano plot all days and network analysis. a. Volcano plot demonstrating proteins differentially expressed in RTT versus iCTR after pooling all time points of neuronal development. The x-axis represents the log2 fold change in abundance (RTT/iCTR) and y-axis the -log10 (p-value). Threshold for

significant proteins is chosen for p- value cutt-off (0.1) and fold change ≤ 1.3. Up regulated proteins in RTT are shown in red and down regulated are shown in blue. b. GO analysis on the Biological Process of the significant proteins. X-axis represents the -Log10 (p-value) and red and blue colors indicate for up and down regulated proteins in RTT respectively. The numbers represent the genes enriched for each term. c. Reactome pathway analysis of the significant proteins. d. Network analysis of the significant proteins by Cytoscape plugin GeneMania. Red indicates for up regulated and blue indicates for down regulated proteins in RTT.

Supplementary Files

This is a list of supplementary files associated with this preprint. Click to download.

- TableS3.xlsx
- TableS2.xlsx
- TableS1.xlsx
- FigureS4.pdf
- FiguresS1.pdf
- TableS4.xlsx
- FigureS2.pdf
- figureX1.pdf
- FigureS3.pdf